Article

Journal of Vibration and Control
1–17

DOI: 10.1177/1077546314560202
jvc.sagepub.com

Influence of temperature on optimum viscoelastic absorbers in cubic nonlinear systems

Mariano Febbo[1], **Eduardo MO Lopes**[2] **and CA Bavastri**[2]

Abstract

Recently, viscoelastic materials have been widely used for vibration control due to their efficacy and flexibility in real engineering problems. Their use as constitutive parts of dynamic vibration absorbers requires the investigation of these materials under different operating situations. In the optimal design of the absorbers, it is essential to know how the dynamical properties of the viscoelastic materials change with temperature. In a previous work, the authors presented a methodology to optimally design a linear viscoelastic dynamic vibration absorber to be attached to a cubic nonlinear single-degree-of-freedom system, in a given temperature. In the present work, a study of how temperature variations affect the optimal design of two viscoelastic absorbers, made of distinct materials (neoprene and butyl rubber), is addressed. The mathematical formulation of the problem is based on the concept of generalized equivalent parameters and the harmonic balance method is employed in the solution stage. A cubic nonlinearity in the primary system is considered and the four parameter fractional derivative model of viscoelastic materials is used. Numerical simulations are performed using a recursive equation, in order to find the new characteristics of the absorbers at different working temperatures. The results show that the answer depends not only on the temperature and the material, but also on the magnitude of the excitation load imposed to the system. For a low magnitude of the excitation load, it is verified that the neoprene absorber is less affected by a temperature variation, in terms of its vibration control capabilities. On the other hand, a large magnitude of the load can significantly affect the performance of both considered devices when the working temperature is different from the design temperature.

Keywords

Cubic non-linear systems, optimum viscoelastic dynamic absorbers, temperature detuning, vibration control

1. Introduction

Widely used in passive vibration control, dynamic vibration absorbers are simple mechanical devices that are used in many systems to reduce the amplitude of vibrations. They work as "absorbing" secondary systems which are attached to another mechanical system, called the primary system, with the purpose of reducing vibration levels of the latter by introducing high mechanical impedance in a frequency region where the primary system needs it. In the past, these devices were used to reduce the rolling motions of ships (Den Hartog, 1956) and over time absorbers have proved themselves extremely efficacious in mitigating vibrations and sound radiation in many structures and machines.

The general theory for the optimum design of absorber systems, when applied to a generic linear structure of any shape, to control each vibration mode, one by one, in a wide frequency band (in equivalence to Den Hartog's theory) was derived by Espíndola and Silva (1992). The theory is based on the concept of generalized equivalent mass and damping parameters for the absorbers. With this concept, it is possible to write down the equations of motion of the compound

[1]Department of Physics, South National University and South Institute of Physics, Bahía Blanca, Argentina
[2]Department of Mechanical Engineering, Federal University of Paraná (UFPR), Brazil

Received: 10 April 2014; accepted: 19 October 2014

Corresponding author:
M Febbo, Department of Physics, South National University and South Institute of Physics (UNS/CONICET)-Avda.Alem 1253, CP 8000, Bahía Blanca, BA, Argentina.
Email: mfebbo@uns.edu.ar

system (primary system plus absorbers) only in terms of the generalized coordinates (degrees of freedom (d.f.)) previously chosen to describe the configuration space of the primary system alone. This is carried out in spite of the fact that the compound system has additional d.f. introduced by the attached absorbers.

This theory has been developed and applied with great success to the optimum design of a linear viscoelastic absorber system, in a large frequency band, where one or more vibration modes are present. This optimal design is made in a simultaneous fashion, by which one or more absorbers are used to control one or more vibration modes, using nonlinear optimization techniques in a modal subspace of the primary system (Espíndola and Bavastri, 1995, 1997; Bavastri, 1997; Bavastri et al., 1998; Espíndola et al., 2005a,c).

Viscoelastic dynamic vibration absorbers (VDVAs) are usually easy to make and apply to a structure of any size and shape. This is in part possible thanks to modern technology of viscoelastic materials and can be verified, for instance, in mitigating vibrations in rotating machines (Doubrawa Filho et al., 2011) and in a notch-type spring mechanism based on the traction principle for tuning fiber Bragg gratings (Neves et al., 2011). Accurate mathematical models are also to be praised. The four parameter fractional derivative model has been successfully employed to describe the dynamic behavior of viscoelastic materials due to its adequacy and its convenient formulation in the frequency domain (Bagley and Torvik, 1979, 1983, 1986; Torvik and Bagley, 1987; Pritz, 1996; Rossikhin and Shitikova, 1998; Lopes, 1998; Espíndola et al., 2005b).

Nonlinear two-d.f. systems have attracted a lot of attention in the past. The reader should refer to Nayfeh and Mook (1979), Schmidt and Tondl (1986), Worden and Tomlinson (2001) and Thomsen (2010) for lists of various studied cases. Of particular concern is the use of nonlinear oscillators as nonlinear dynamic vibration absorbers (NDVAs) or nonlinear tuned mass dampers. The contributions of Roberson (1952), Pipes (1953), Soom and Lee (1983) and Nissen et al. (1985) are highlighted. Their strategy to approach the problem was to use approximation methods (Ritz or harmonic balance) to obtain the steady-state solutions and then optimize the NDVAs for vibration reduction purposes. Recently, several works on optimal linear control for strongly nonlinear systems has been proposed to diminish chaotic (Nozaki et al., 2013) or impact (Costa and Balthazar, 2009) oscillations.

Several nonlinear phenomena can be found in systems of the above type, such as jumps, saturation and types I and II intermittency, as well as periodic and periodically and chaotically modulated motions (Oueini et al., 2000). These nonlinear phenomena depend on the parity character of the nonlinearity and can be used differently for vibration control. For instance, the application of the saturation phenomenon (discovered in quadratic nonlinear systems by Nayfeh in 1973) showed that vibrations could be suppressed in a wide range of frequencies in nonlinearly coupled systems with two-to-one internal resonance (Ashour and Nayfeh, 2003). For systems with cubic nonlinearities, the papers of Rice (1986) and Shaw et al. (1989) pointed out the possibility of a combination-type instability, which is detrimental for vibration control due to the appearance of quasi-periodic oscillations of large vibration amplitudes. Natsiavas (1992) further studied the same phenomenon finding out that a proper selection of the system parameters could avoid the quasi-periodic solutions, which could have dangerous effects. A novel type of nonlinear vibration absorber of finite extensibility (odd type parity of nonlinearity) was proposed by Febbo and Machado (2013), showing a better effectiveness for a large nonlinearity in the primary system when compared with a cubic nonlinear absorber. Also the use of another type of nonlinear absorber, shock absorbers, has been proven to be effective to improve comfort in passenger vehicles (Silveira et al., 2014).

Targeted energy transfer (TET) in two-d.f. systems comprising a linear primary system and a nonlinear attachment has been carefully investigated in the field of vibration control (Vakakis et al., 2008). It was demonstrated that at certain ranges of parameters and initial conditions, passive TET makes it possible for vibration energy initially localized in the linear oscillator to get passively transferred to the attachment in an almost irreversible way (Kerschen et al., 2006). Most of these models consider a stiff cubic nonlinear spring and a linear damper attached to the primary system, but recently the use of nonlinear attachments with non-polynomial characteristics has also been studied (Gendelman, 2008). Tusset et al. (2013) applied active and passive control to suppression of chaotic behavior in a non-ideal portal frame structural system. The active control consists of a nonlinear feedforward and feedback control, whereas the passive one was obtained by means of a nonlinear energy sink. An overview of the dynamical coupling between energy sources and structural response can be viewed in Balthazar et al. (2003).

Linear vibration absorbers have also been considered for vibration control of nonlinear primary systems. Among those, a two-d.f. system comprising a weakly nonlinear primary system and a linear absorber was presented by Ji and Zhang (2010) and Ji (2012), with the aim of studying the effectiveness of the linear absorber in suppressing resonance vibrations. With the exception of their previous work (Bavastri et al., 2013), the authors are not aware of other cases of the use of linear viscoelastic absorbers to mitigate vibrations in nonlinear systems.

It is well-known that the dynamic properties of viscoelastic materials change, in a more or less pronounced way, when the temperature changes. In Bavastri et al. (2013), a methodology was presented for the optimal design of a dynamic viscoelastic absorber acting in a cubic nonlinear system (Duffing type oscillator) at a given temperature. The aim of the current paper is to review the methodology proposed there and to study the influence of temperature variations on the optimal design.

This paper is organized as follows. In the next section, a brief review on the characteristics of a VDVA based on the four parameter fractional derivative model and on the concept of generalized equivalent parameters is made. Then, the full mathematical model is presented along with a brief description of the optimization strategy. After that, the numerical results regarding the effectiveness of the proposed control strategy under temperature variations are supplied. Two distinct viscoelastic materials are considered in the investigation and also two different values of the magnitude of the excitation load. Finally, concluding remarks are offered.

2. Viscoelastic dynamic vibration absorbers

Figure 1 shows a particular ordinary absorber (neutralizer). In between its rigid mass m_a and its base lies a viscoelastic spring which is a piece of viscoelastic material, sometimes with some metal inserts. The base is used to attach the absorber to the system to be controlled, called herein the primary system.

This is in fact a single-d.f. VDVA. The stiffness constant of the viscoelastic spring, in the frequency domain, is given by (Espíndola and Silva, 1992)

$$k_s(\Omega, T) = \vartheta G_c(\Omega, T) \tag{1}$$

In equation (1), $G_c(\Omega, T)$ is the so-called complex shear modulus of the viscoelastic material, which is frequency, Ω, and temperature, T, dependent. Also in equation (1), ϑ is a geometric constant depending on the shape of the viscoelastic spring and of its metal inserts.

In terms of the four parameter fractional derivative model for a viscoelastic material (Pritz, 1996), $G_c(\Omega, T)$ may be expressed as

$$G_c(\Omega, T) = \frac{G_0 + G_\infty (ib\Omega)^\beta}{1 + (ib\Omega)^\beta} \tag{2}$$

where $i = \sqrt{-1}$ is the imaginary unit
or

$$G_c(\Omega, T) = \frac{G_0 + G_\infty \varphi_0 [i\alpha_T(T)\Omega]^\beta}{1 + \varphi_0 [i\alpha_T(T)\Omega]^\beta} \tag{3}$$

where G_0 and G_∞ are the low and upper asymptotes, respectively, β is the fractional order of the derivative appearing in the constitutive differential equation of the viscoelastic material and b is the relaxation time constant of the material.

The relaxation time is highly sensitive to temperature and is usually expressed as $b = \alpha_T(T) b_0$, where b_0 is b computed at the so-called reference absolute temperature T_0 and $\alpha_T(T)$ is known as the shift factor. With $\varphi_0 = b_0^\beta$, it is verified that equation (3) results from equation (2). The shift factor can be computed by $\alpha_T(T) = 10^{-\theta_1 (T - T_0)/(\theta_2 + T - T_0)}$, where θ_1 and θ_2 are constants to be determined experimentally. This empirical expression, consistent with experience and known as the William-Landel-Ferry (WLF) equation, can be found in Ferry (1980).

It is also appropriate to write the complex shear modulus in the form

$$G_c(\Omega, T) = G(\Omega, T)[1 + i\eta_G(\Omega, T)] \tag{4}$$

where $G(\Omega, T)$ is the real part of the complex shear modulus, known as the dynamic shear modulus, and $\eta_G(\Omega, T)$ is the corresponding loss factor. The loss factor is the ratio of the imaginary part of the complex shear modulus to its real part and measures the ability of the material to convert energy of deformation into heat.

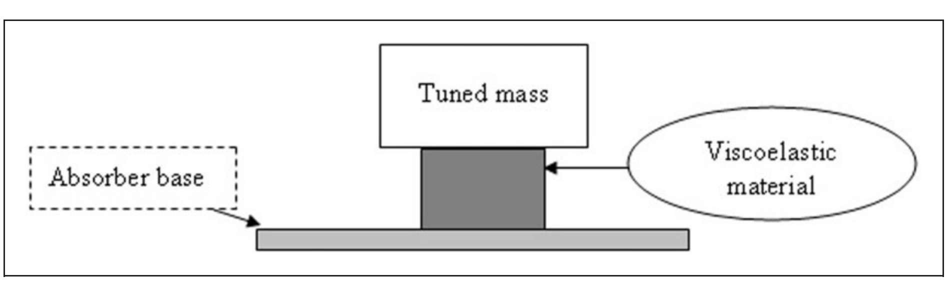

Figure 1. A simple viscoelastic dynamic absorber.

It is useful to write down explicitly the real part of the complex shear modulus $G(\Omega, T)$ and the loss factor $\eta_G(\Omega, T)$ to stress their temperature dependence. They are

$$G(\Omega,T) = \frac{G_0 + (G_0 + G_\infty)\varphi_0\alpha_T(T)^\beta\Omega^\beta\cos\left(\beta\frac{\pi}{2}\right) + G_\infty\varphi_0^2\alpha_T(T)^{2\beta}\Omega^{2\beta}}{1 + 2\varphi_0[\alpha_T(T)\Omega]^\beta\cos\left(\beta\frac{\pi}{2}\right) + \varphi_0^2\alpha_T(T)^{2\beta}\Omega^{2\beta}} \quad (5)$$

and

$$\eta_G(\Omega,T) = \frac{(G_\infty - G_0)\varphi_0[\alpha_T(T)\Omega]^\beta\sin\left(\beta\frac{\pi}{2}\right)}{G_0 + (G_0 + G_\infty)\varphi_0[\alpha_T(T)]^\beta\cos\left(\beta\frac{\pi}{2}\right) + G_\infty\varphi_0^2\alpha_T(T)^{2\beta}\Omega^{2\beta}} \quad (6)$$

where the temperature dependence is introduced by the shift factor $\alpha_T(T)$, via the WLF equation.

3. Equivalent generalized quantities for an absorber

As shown in Espíndola and Silva (1992) and also seen in Bavastri et al. (2013), an equivalent model of the secondary system, obtained by its equivalent generalized parameters, can be found through the complex rigidity on its base, $k_a(\Omega, T)$. The secondary system, as a simple absorber at a given constant temperature, is dynamically depicted in Figure 2, in correspondence with the previous view of Figure 1. It has a single lump of mass m_a connected to the primary structure through a resilient device (“spring”) assumed as having a viscoelastic nature. From equations (1) and (4), it is observed that its complex stiffness $k_s(\Omega, T)$ for any given temperature, is supplied by (Espíndola and Silva, 1992)

$$k_s(\Omega, T) = \vartheta G_c(\Omega, T) = \vartheta G(\Omega, T)[1 + i\eta_G(\Omega, T)] \quad (7)$$

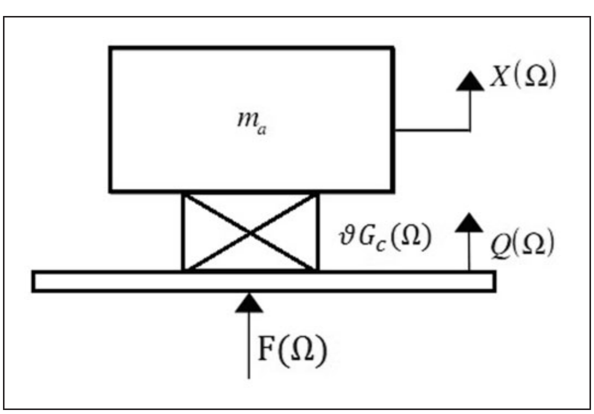

Figure 2. Scheme of a simple (one-degree-of-freedom) absorber.

In Figure 2, the base is assumed massless and $Q(\Omega)$ and $F(\Omega)$ stand, respectively, for the Fourier transform of the base displacement, $q(t)$, and the applied force, $f(t)$, at a certain temperature. This applied force results from the interaction between the absorber and the point of the primary structure where the absorber is attached.

It can be verified that the primary structure “feels” the neutralizer at the attachment point, at the temperature of concern, as a dynamic stiffness given by

$$k_a(\Omega, T) = \frac{F(\Omega, T)}{Q(\Omega, T)} = \frac{m_a\Omega^2\vartheta G_c(\Omega, T)}{m_a\Omega^2 - \vartheta G_c(\Omega, T)} \quad (8)$$

In terms of equivalent quantities, the dynamic stiffness given above can be rewritten as

$$k_a(\Omega, T) = -\Omega^2 m_e(\Omega, T) + i\Omega c_e(\Omega, T) \quad (9)$$

Then, by considering equations (7)–(9), the generalized equivalent parameters for the absorber can be obtained as (Espíndola and Silva, 1992; Bavastri et al., 2013)

$$c_e(\Omega, T) = m_a\Omega_a \frac{r_a(\Omega, T)\eta(\Omega, T)\varepsilon_a^3}{\left(r_a(\Omega, T) - \varepsilon_a^2\right)^2 + (r_a(\Omega, T)\eta(\Omega, T))^2} \quad (10)$$

and

$$m_e(\Omega, T) = m_a \frac{r_a(\Omega, T)\left[r_a(\Omega, T)\left(1 + \eta^2(\Omega, T)\right) - \varepsilon_a^2\right]}{\left(r_a(\Omega, T) - \varepsilon_a^2\right)^2 + (r_a(\Omega, T)\eta(\Omega, T))^2} \quad (11)$$

where $\varepsilon_a = \frac{\Omega}{\Omega_a}$ and $r_a = \frac{G(\Omega, T)}{G(\Omega_a, T)}$, both for any given temperature.

As to the characteristic frequency (also called natural or anti-resonant frequency), Ω_a, it is defined for a simple absorber as the one which, in the absence of damping, makes the denominator of equation 8 equal to zero. That is,

$$\Omega_a^2 = \frac{\vartheta G(\Omega_a, T)}{m_a} \quad (12)$$

where $\vartheta G(\Omega_a, T)$ is the stiffness of the viscoelastic spring at the characteristic frequency Ω_a and the temperature T. It is noted that equation (12) is a transcendental equation for the characteristic frequency of the absorber.

Observing equation (9), it can be said that, at any given temperature T, the primary structure ‘‘sees’’ the absorber at the point of attachment as a mass $m_e(\Omega)$ connected in series to a viscous dashpot of constant $c_e(\Omega)$, the other end of which is connected to the ‘‘earth’’. Figure 3 shows this interpretation. These two quantities are called generalized equivalent mass and generalized equivalent viscous damping constant, respectively, for a particular absorber.

The dynamics of the compound system (primary + absorber) can thus be formulated in terms of the original physical generalized coordinates alone (of which $Q(\Omega)$, in Figure 3, is representative), although the new system now has additional d.f. (one for each absorber, if more than one is present). This is the main advantage of the concept of generalized equivalent parameters as far as the absorbers are concerned. It is important for the optimization design of the absorber to work with the dynamic equivalent model shown in Figure 3.

4. Mathematical formulation

The whole mechanical system to be modeled is equal to the one analyzed in Bavastri et al. (2013) and can be observed in Figure 4(a), while the corresponding equivalent system, using the concept of equivalent generalized parameters, is presented in Figure 4(b). The system to be controlled (hereafter the primary system) is nonlinear with an odd-cubic type nonlinearity (Duffing oscillator). Attached to it and acting as the control system there is a linear VDVA. Using the equivalent generalized parameters, the equation of motion of the primary system is given by

$$[m_1 + m_e(\Omega, T)]\ddot{x}_1 + k_1 x_1 + k_{1NL} x_1^3 + [c_1 + c_e(\Omega, T)]\dot{x}_1 = f\cos(\Omega, T) \tag{13}$$

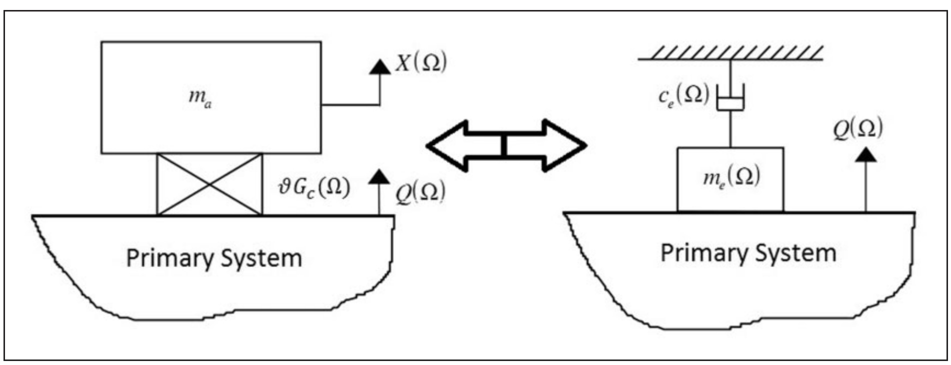

Figure 3. Equivalent systems.

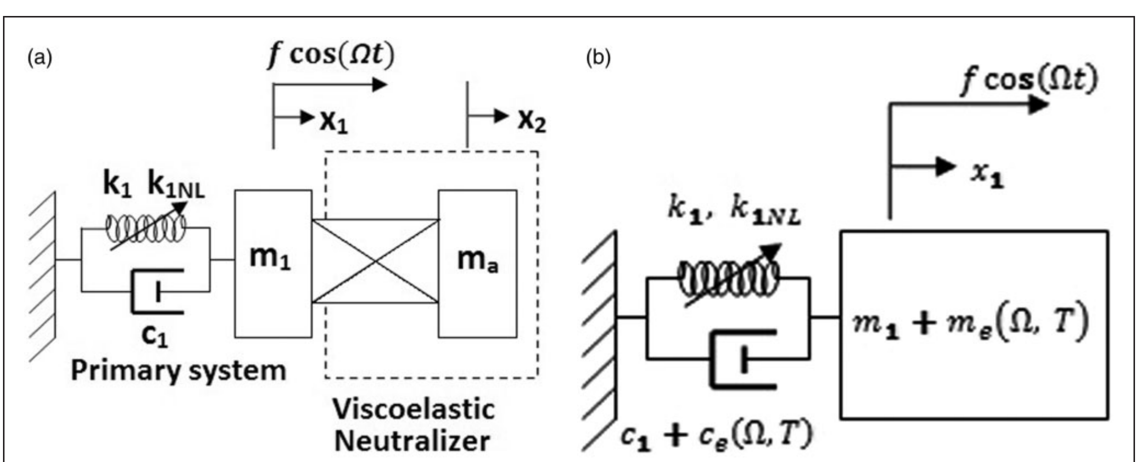

Figure 4. (a) Compound system under study; (b) Compound system with generalized equivalent parameters.

where m_1 and $m_e(\Omega, T)$ are, respectively, the mass of the primary system and the equivalent mass of the neutralizer, which is given by equation (11) and includes both the temperature and the frequency dependencies. The parameters k_1, k_{1NL} and c_1 denote, in their turn, the linear and nonlinear values of stiffness (acting in parallel) and the damping constant (considered of viscous type) of the primary system. Lastly, there is $c_e(\Omega, T)$, which is the equivalent damping of the neutralizer, given by equation (10) and also includes the effects of temperature and frequency.

In the following text, the authors will use the derivation given in Bavastri et al. (2013). For the sake of brevity, that procedure will be presented herein in a condensed form.

Dividing equation (13) by m_1 and introducing the parameters

$$\omega_{10} = \sqrt{\frac{k_1}{m_1}}, \quad \alpha = \frac{k_{1NL}}{m_1}, \quad \mu_e(\Omega, T) = \frac{m_e(\Omega, T)}{m_1},$$
$$\mu = \frac{m_a}{m_1}, \quad f_0 = \frac{f}{m_1}, \quad \lambda_1 = \frac{c_1}{m_1}, \quad \lambda_e(\Omega, T) = \frac{c_e(\Omega, T)}{m_1}$$

the equation of motion turns out to be

$$[1 + \mu_e(\Omega, T)]\ddot{x}_1 + \omega_{10}^2 x_1 + \alpha x_1^3 + [\lambda_1 + \lambda_e(\Omega, T)]\dot{x}_1 = f_0 \cos(\Omega, T) \tag{14}$$

Assuming an approximate stationary solution of the system as $x_1(t) = a\cos(\Omega, T)$ it is possible to obtain a frequency response curve (FRC) by the harmonic balance method (Nayfeh and Mook, 1979). This FRC gives the vibration amplitude a bythe following equation:

$$a^2\left\{\omega_{10}^2 - \Omega^2[1 + \mu_e(\Omega, T)] + \alpha\frac{3}{4}a^2\right\}^2 + [\lambda_1 + \lambda_e(\Omega, T)]^2\Omega^2 a^2 = f_0^2 \tag{15}$$

5. Optimization strategy

The optimal parameters of the VDVA are achieved using nonlinear optimization techniques. Denoting the vibration amplitude of the primary system, a, for a given constant temperature, as $H(\Omega)$, the objective function is given by

$$f_{obj}(x) : R^n \rightarrow R = \|H(\Omega, x)_{\Omega_1 \leq \Omega \leq \Omega_2}\|_F \tag{16}$$

where $\|\cdots\|_F$ represents the Frobenius norm, Ω_1 and Ω_2 are the low and upper limits of the frequency band of interest, respectively, and x is the design vector. The aim here is to reduce as much as possible the amplitude of the displacement of the primary system when the optimal absorber is attached to it. That is, the procedure seeks to find an x that corresponds to the smallest value of a for the considered frequency range ($\Omega_1 \leq \Omega \leq \Omega_2$). It is stressed that, over the optimization process, a certain temperature is chosen and it is kept constant.

The design vector in this particular case is defined as

$$x = \Omega_a \tag{17}$$

where Ω_a is the characteristic (natural) frequency of the absorber.

In this work, the Nelder-Mead method is used as the nonlinear optimization technique. Inequality or equality constraints for the design vector are not employed. Both the solution of the nonlinear problem, $H(\Omega, x)$, and the nonlinear optimization technique were implemented by the authors in the Matlab environment.

The optimal characteristic frequency, Ω_a^*, follows from the optimization procedure. Then, with m_a equalto 0.15 m_1 (Den Hartog's theory), the geometric factor of the VDVA, ϑ, is calculated from equation (12). Finally, to achieve the physical realization of the VDVA, the procedure described in Espíndola et al. (2009, 2010) should be followed.

6. Recursive method for a new characteristic frequency

Conceptually, when a viscoelastic dynamic absorber is designed in optimal form, it introduces high mechanical impedance around its characteristic frequency in the host (primary) system. Then, it can reduce the vibration amplitude of the primary system to acceptable levels.

Depending on the operating region, the viscoelastic material can be highly temperature and frequency dependent. Thus, a small temperature variation implies a high variation of the dynamic shear modulus which can make the characteristic frequency of the absorber change considerably. This situation can lead to a detuning of the absorber, causing a non-optimum performance.

When this detuning happens, the new characteristic frequency in the new working temperature can be found from equation (12) in a recursive form. This is achieved by a numerical code whose input parameters are the original characteristic frequency of the absorber and the new working temperature. Given these parameters, a new value for the dynamic shear modulus can be found (see equation (5)) and then, as the parameters ϑ and m_a are fixed (once the absorber has already been built), a new value for the characteristic frequency can be computed from equation (12). This process is repeated until convergence happens, that is, until the characteristic frequency and the dynamic shear modulus, calculated at the same characteristic frequency, agree. When this condition is attained, the final value for the characteristic frequency of the absorber, at the new working temperature, is achieved.

This modified characteristic frequency is employed in the numerical simulation to show the influence of the temperature on the quality of the passive control performed by the viscoelastic dynamic absorber.

7. Numerical examples and discussion

This section encompasses the results corresponding to the steady-state solutions of a nonlinear primary system with two different VDVAs attached to it, one containing neoprene and the other butyl rubber. These steady-state solutions were determined by equation (14).

To perform the stability analysis of the periodic solutions, a variational approach was employed, as can be observed, for instance, in Thomsen (2010), Zhu et al. (2004) and Schmidt and Tondl (1986). This consisted of obtaining linear perturbed equations from the solutions of equation (13) and then judging the eigenvalues of the determinant of the matrix coefficients. If the real part of all the eigenvalues is negative, then the periodic solution is stable; otherwise, it is unstable. If a real value changes sign, it is a saddle-node bifurcation and can result in a jump of the solution. On the other hand, if there is a pair of complex conjugate eigenvalues whose real part changes sign, a Hopf bifurcation results and the system exhibits quasi-periodic solutions. It must be pointed out that the considered two-d.f. nonlinear systems can exhibit, for example, saddle-node bifurcations, Hopf bifurcations, and chaos. The emergence of a Hopf bifurcation, which frequently appears in two-d.f. nonlinear systems for a certain selection of system parameters (see Natsiavas, 1992, Shaw et al., 1989, Gendelman, 2008, Vakakis et al., 2008), can result in large vibration amplitudes, due to the presence of stable quasi-periodic solutions. Chaotic solutions in two-d.f. nonlinear systems are observed in passive vibration control, as demonstrated by Febbo and Machado (2013).

The current analysis is based on the study of the behavior of the viscoelastic absorbers when the working temperature changes with respect to the design temperature, which was arbitrarily selected as 303 K. This design temperature was the one employed to optimize the viscoelastic absorbers, as explained previously. The study also analyzes the influence of the magnitude of the excitation load on the behavior of the compound system for the distinct considered temperatures. The frequency range was limited to approximately 6 Hz to 24 Hz, but other frequency ranges could be considered following the same general procedure. The temperature range was ± 30 K around the design temperature, that is, it was from 273 K to 333 K.

As mentioned above, two types of viscoelastic materials were selected for carrying out this study: neoprene and butyl rubber. They were chosen because they are usually employed in vibration control devices and present different behaviors under temperature variation. These can be seen in the corresponding nomograms, given in Figures 5 and 6, which display the dynamic shear modulus and the corresponding loss factor as functions of frequency and temperature. The nomograms, as usual, also contain a horizontal axis for the reduced frequency, which is the product between the shift factor $\alpha_T(T)$ and the frequency.

As is known for materials with thermorheologically simple behavior, three different regions can be distinguished in the nomograms: type I, II and III regions (Snowdon, 1968). Type I region is called the rubbery region and is characterized by a near constant dynamic shear modulus and a moderate loss factor. In type II region, also known as the transition region, the maximum loss factor occurs and the dynamic shear modulus changes most rapidly. Type III region is called the glassy region and it is where the material becomes brittle and the loss factor is fairly low (Nashif et al., 1985). The material, in this region, is undesirable for vibration control purposes.

From the information provided by Figure 5, it can be observed that, at the design temperature and the considered frequency range, the neoprene works in the limit between type I and type II regions. Its dynamic shear modulus is practically constant in this case and the loss factor is relatively low. Thus, when the material experiences a moderate temperature change, the dynamic shear modulus keeps on approximately the same value as the loss factor varies in a more significant way. On the other hand, Figure 6 shows that, given the same conditions, the butyl rubber has its dynamic shear modulus strongly dependent on temperature and frequency, with its loss factor close to its maximum value. As mentioned before, this is typical of materials in type II region.

Table 1 shows the physical parameters of the four parameter fractional derivative models corresponding to the two abovementioned viscoelastic materials. The complementary parameters, which account for the variation of temperature according to the WLF equation, are displayed in Table 2.

The other data employed in this study were: $m_1 = 1$ kg; $m_a = 0.15$ kg; $\omega_{10} = 73.01$ rad/s; $f_{10} = 11.62$ Hz; $\alpha = 5$ N/mkg; $\lambda_1 = 0.1$Ns/mkg; $\Omega_1 = 40.0$ rad/s; $f_1 = 6.37$ Hz; $\Omega_2 = 150.8$ rad/s and $f_2 = 24$ Hz. As to the magnitude of the applied load, two values were investigated: $f_0 = 1000$ N/kg and $f_0 = 10000$N/kg.

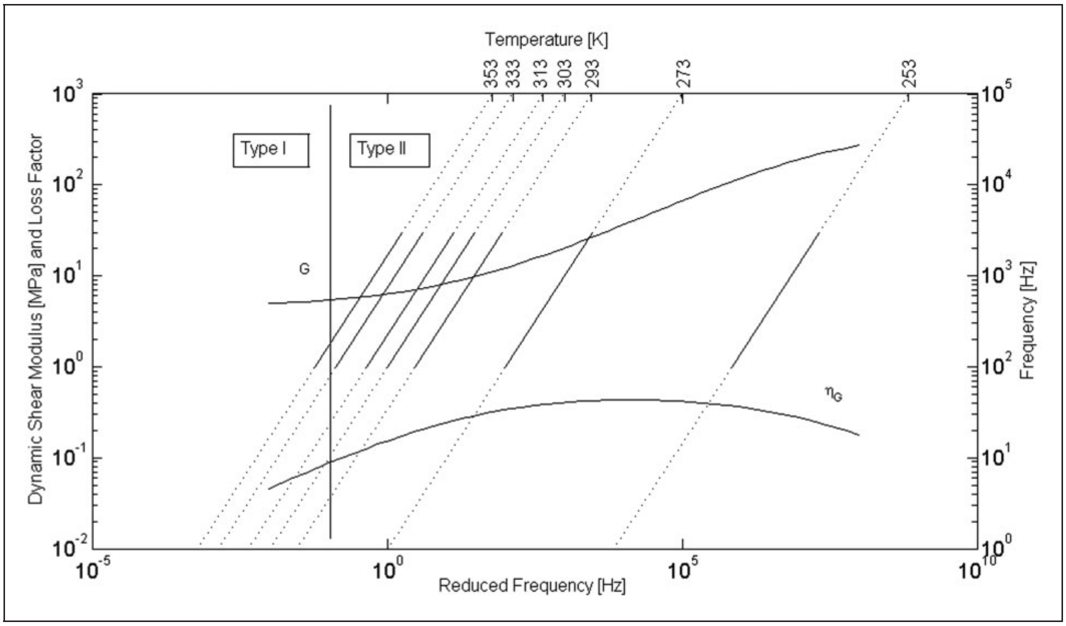

Figure 5. The nomogram of neoprene.

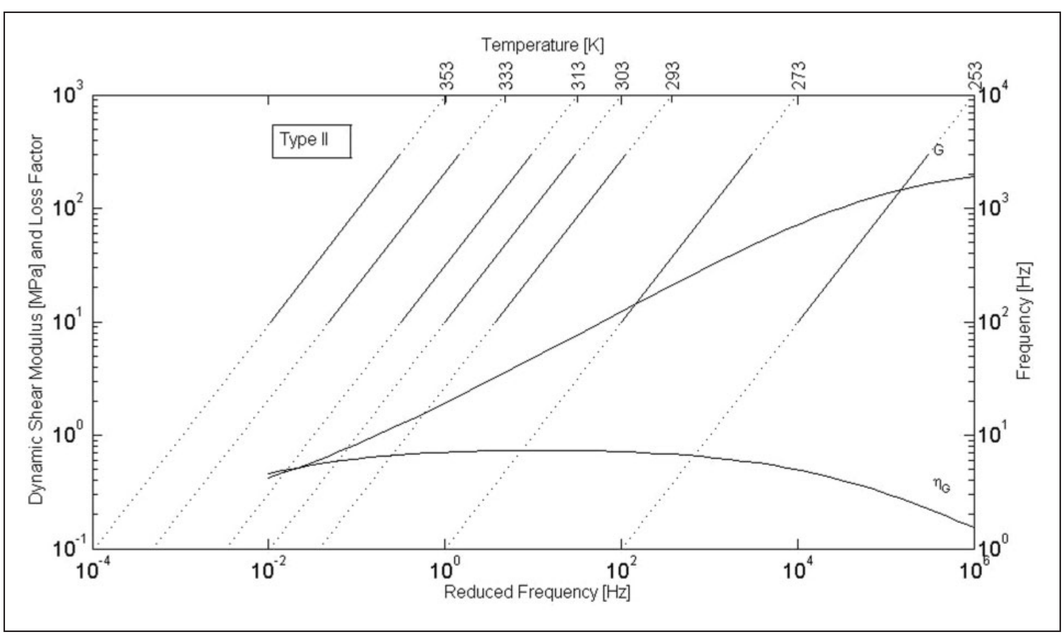

Figure 6. The nomogram of butyl rubber.

Table 3 shows the characteristic frequencies of the neoprene VDVA and the butyl rubber VDVA for different working temperatures around the design temperature, which was used for the optimal design of the absorbers. In this case, the nonlinear parameters are $\alpha = 5$ and $f_0 = 1000$ for the sake of comparison with the authors' previous work (Bavastri et al., 2013). As a distinguished feature, a much more pronounced variation of the characteristic frequency can be observed for the butyl rubber absorber than for the neoprene absorber when the temperature changes. Table 4 shows similar results considering $\alpha = 5$ and

Table 1. Model parameters of neoprene and butyl rubber.

Material type	$G_0(N/m^2)$	$G_\infty(N/m^2)$	β	$\varphi_0 = b_0^\beta$
Neoprene	4.55e6	4.18e8	0.319	0.00274
Butyl rubber	1.76e5	2.41e8	0.424	0.00424

Table 2. Complementary parameters of neoprene and butyl rubber.

Material type	θ_1	θ_2	T(K)	T_0(K)
Neoprene	5.09	46.5	303	273
Butyl rubber	9.91	119	303	273

Table 3. Characteristic frequencies at different temperatures with $\alpha = 5$ and $f_0 = 1000$.

Temperature (K)	Characteristic frequencies of the absorber (Hz)	
	Neoprene	Butyl rubber
273	13.88	28.94
283	12.10	18.48
293	11.37	12.73
303*	10.99*	9.70*
313	10.78	7.85
323	10.65	6.74
333	10.56	6.05

*design temperature and optimal frequencies.

Table 4. Characteristic frequencies at different temperatures with $\alpha = 5$ and $f_0 = 10000$.

Temperature (K)	Characteristic frequencies of the absorber (Hz)	
	Neoprene	Butyl rubber
273	14.77	29.96
283	12.86	19.14
293	12.07	13.31
303*	11.67*	10.03*
313	11.44	8.11
323	11.29	6.95
333	11.20	6.21

*design temperature and optimal frequencies.

$f_0 = 10000$. Clear differences are also observed there, given the detuning suffered by both absorbers, in a similar way to that of Table 3.

Figure 7 shows the results of the optimization process for the neoprene VDVA and the influence of temperature in the optimization results. In this figure, the values of $\alpha = 5$ and $f_0 = 1000$ were considered. For the sake of clarity in the interpretation of the results, the solid lines represent the stable solutions as the dashed lines the unstable ones. Both the primary system FRC and the compound system FRCs at different temperatures are displayed.

It can be observed in Figure 7 that, as the characteristic frequency of the neoprene VDVA changes with temperature, that is, as detuning occurs, different FRCs are generated. Generally speaking, detuning would deteriorate the absorber performance as the characteristic frequency would no longer be optimal. This is verified in this particular case when the temperature rises, as the neoprene goes from the limit between type II and type I regions to type I region (see Figure 5). The dynamic shear modulus is still approximately constant but the loss factor continuously decreases from its value at the design temperature.

However, on the other hand, when the temperature reduces, the dynamic characteristics of this material "walk" in the direction of type II region (see also Figure 5), showing a significant increase in the loss factor, and hence in the capability of dissipating vibration energy, along with a moderate increase in the dynamic shear modulus. Then, the absorber performance progressively improves regarding the optimal case. This makes it clear that the characteristic frequency is strictly optimal at the design temperature, which, in its turn, is not the most favorable for the considered viscoelastic material.

However, all the compound system solutions remain stable, despite the nonlinear character of the primary system, which is remarkable. Moreover, there was not a single case in which evidence of a Hopf bifurcation resulting in quasiperiodic motions was observed. To account for the evidence of chaos, a large number of numerical simulations was performed, with several initial conditions, for all the considered cases and the whole set of corresponding frequencies. At the end of this procedure, no evidence of chaotic solutions was obtained.

Figure 8 shows the results for the butyl rubber VDVA, for the same cases depicted in Figure 7. As the temperature rises, the absorber performance increasingly deteriorates but the character of a two-d.f. compound system can still be observed. Nevertheless, for temperatures below the design temperature, as the butyl rubber goes deeper in the transition (type II) region (see Figure 6), the system turns to

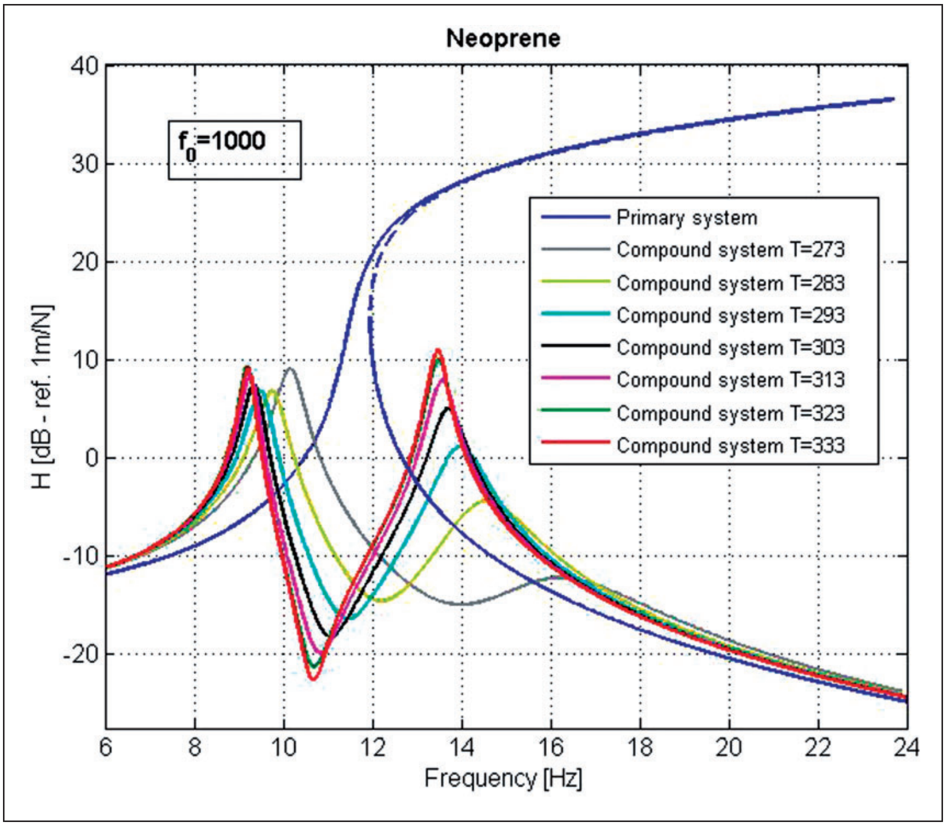

Figure 7. $H(\Omega)$ of the primary and the compound systems with neoprene VDVA at different temperatures, with $f_0 = 1000$, and $\alpha = 5$.

behave as a damped single-d.f. system. This is due to the combined changes in the dynamic shear modulus and in the loss factor, which also cause the absorber to be more and more ineffective.

As an extreme feature of these results, it is possible to observe that a large reduction of temperature results in a variation of the stability character of the solution (stable to unstable), with the compound system approaching the behavior of the primary system. However, only instabilities of a saddle-node type have been observed. The same procedure applied to the neoprene case was employed in this case and no evidence of a Hopf bifurcation or even chaotic solutions was observed.

To investigate the effect of variation of the magnitude of the excitation load, the same calculations employed to generate Figures 7 and 8 were performed again, now keeping fixed the value of the nonlinear parameter α (that is, $\alpha = 5$), but considering a different (large) magnitude of the load $f_0 = 10000$. It is noted that this new magnitude of the excitation load almost trebled the value of the frequency at which the jump occurs for the primary system in an upward sweep (according to the numerical calculations, $f_p^j = 70.52\,\text{Hz}$, as in Figure 9(b), compared to $f_p^j = 23.64\,\text{Hz}$, as in Figure 7, with $f_0 = 1000$).

The results regarding the neoprene absorber are depicted in Figure 9(a) and (b). It can be seen immediately in those figures that the vibration amplitudes of the compound system are larger than those noted in Figure 7. Clearly, this is attributable to the larger magnitude of the excitation load.

It should be also highlighted that the compound system is now completely stable only at 283 K and 293 K. At all the other temperatures, the compound system changed its behavior and the corresponding solutions present instabilities (which occasionally may not be perfectly clear in Figure 9(a)).This loss of stability is due to the appearance of saddle-node bifurcations, resulting in jumps in the solutions.

Another important feature can be observed in Figure 9(b), which is a zoomed out view of Figure 9(a), introduced to highlight the frequency values of the jumps at upward sweeps for the three largest temperatures (313 K, 323 K and 333 K). For these temperatures, the results clearly show that even when the VDVA is not capable of achieving a great vibration reduction, it still shows some benefits when compared to the system without the absorber, almost halving the jump frequency in the worst case ($T = 333\,\text{K}$). The reduction of jump frequencies in strong nonlinear systems is

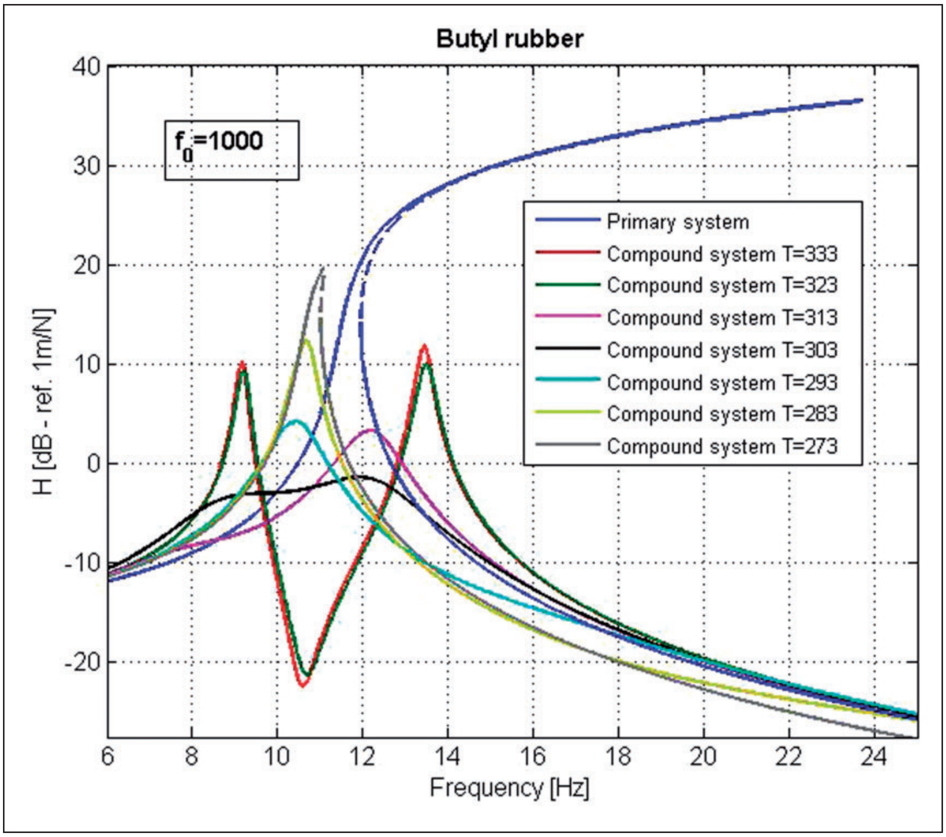

Figure 8. $H(\Omega)$ of the primary and the compound systems with butyl rubber VDVA at different temperatures, with $f_0 = 1000$, and $\alpha = 5$.

very important because it prevents the system having a stable solution of very large amplitude over a long frequency range.

From the stability analysis, it was also verified that there was no evidence of quasi-periodic motions in the considered frequency range or even chaotic solutions, similar to the other cases of lower magnitude of the excitation load, which is remarkable.

Figure 10 shows the influence of temperature changes with regard to the butyl rubber absorber, when considering $f_0 = 10000$. As previously remarked on, the butyl rubber works in the type II region, where the damping is high and the dynamic modulus strongly depends on temperature. However, a decrement in damping can be observed when the temperature increases from the design temperature (see Figure 6).

Analyzing the results for the different temperatures, it is noted that the compound system shows no specific evidences of nonlinear behavior at the design temperature of 303 K only. At the other temperatures, distortions around the peaks and instabilities can be clearly seen. The instability at 273 K, already noticed in Figure 8, is now more pronounced. As for 323 K and 333 K, a particular remark should be made. It was already pointed out that the large magnitude of the excitation load made the peak amplitude of the primary system to appear at $f_p^j = 70.52$ Hz (see Figure 9(b)). Hence, the resonance peak is, for $f_0 = 10000$, far apart from the resonance peak of Figure 8, implying that the butyl rubber VDVA at 323 K and 333 K (with resonant frequencies of $f_{323} = 6.95$ Hz and $f_{333} = 6.21$ Hz, as seen in Table 4) is extremely detuned. So, the system "mimics" the response of a lightly damped single-d.f. nonlinear system.

Similar to the previous case, of a neoprene VDVA, no evidences of quasi-periodic motions or chaotic motions were observed.

8. Higher harmonics in the solution

It is relevant to this study to know if the dynamic response of the system, modeled by equation (13), has only one harmonic in the solution, as assumed by equation (15). To this end, the authors numerically solved equation (13) for a set of selected cases, with a standard ordinary differential equation solver (using Matlab). Obviously, the obtained solution is free of any

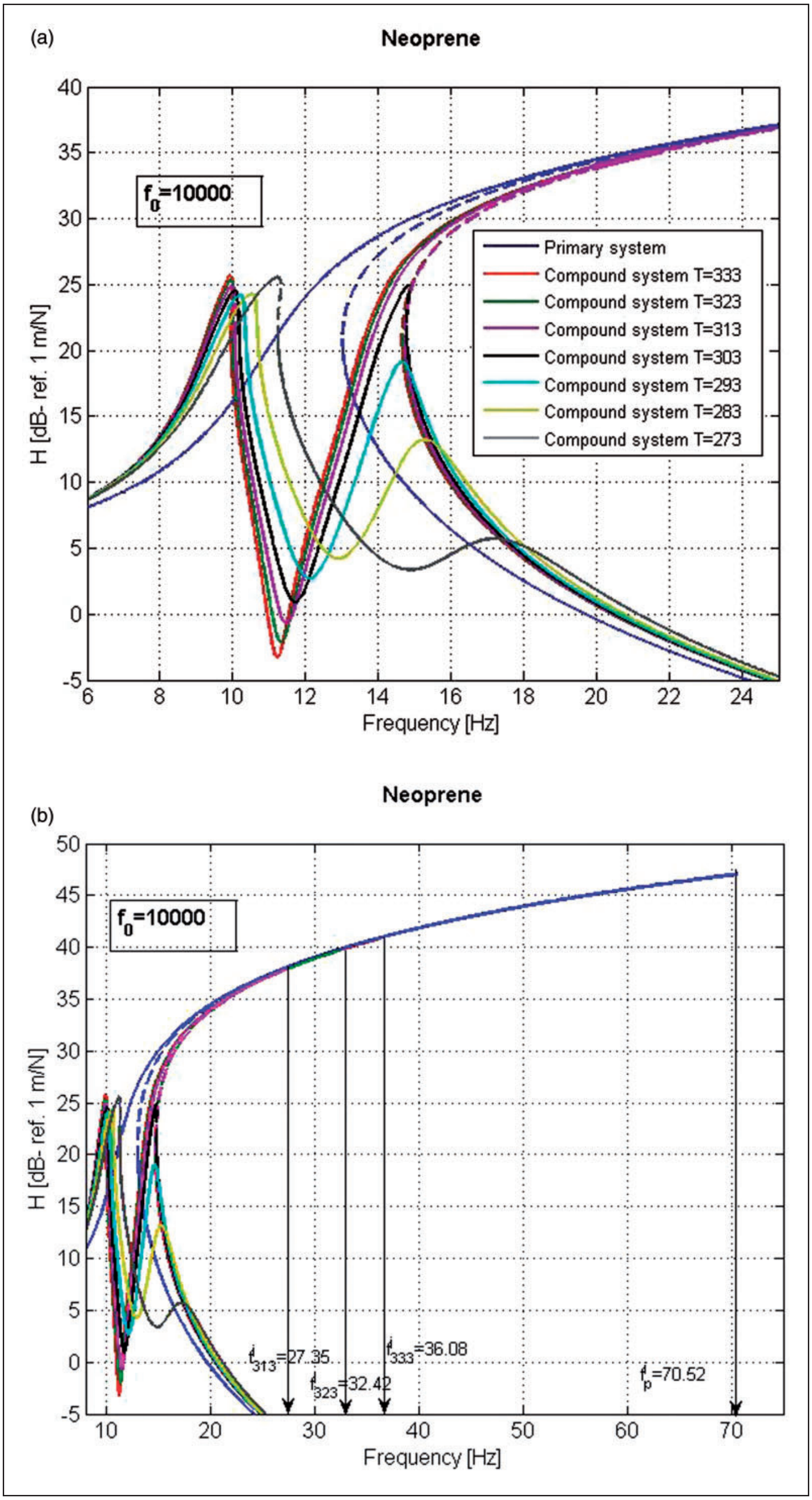

Figure 9. (a) $H(\Omega)$ of the primary and compound systems with neoprene VDVA at different temperatures, with $f_0 = 10000$, and $\alpha = 5$. (b) Enlargement of (a) to see the jump frequencies for the compound system at $T = 313$ K, 323 K and 333 K, and for the primary system.

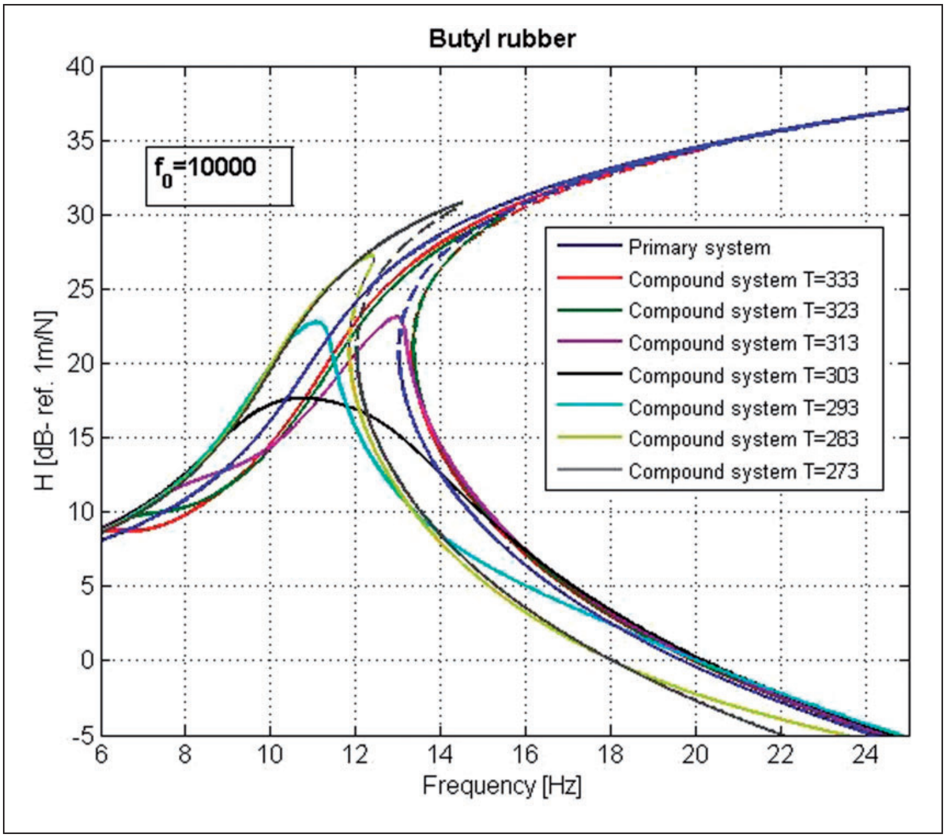

Figure 10. $H(\Omega)$ of the primary and compound systems with butyl rubber VDVA at different temperatures, with $f_0 = 10000$ and $\alpha = 5$.

assumption. Figures 11(a)(b) and 12(a)(b) show the results. For the sake of brevity, we have selected the cases in which the nonlinearity is more significant.

In Figure 11 we have selected the case of a neoprene VDVA with $f_0 = 10000, \alpha = 5$ and $= 333\,\text{K}$. The driven frequency was selected to be 27.06 Hz. In Figure 11(a) we show the time domain solution of the compound system which corresponds to the high amplitude solution of the second upper arm of the FRC of Figure 9 (red color). Now, if we compute the spectrum, we can see in Figure 11(b) that the first harmonic is at least 20 times larger than the third harmonic (that appears as a consequence of the cubic nonlinearity), as its contribution is negligible in the total response.

Finally, we illustrate another emblematic case for butyl rubber. We have also selected the case of $f_0 = 10000, \alpha = 5$ and $T = 333\,\text{K}$. This time the excitation frequency was 18.27 Hz and the results are shown in Figure 12.

In Figure 12(a) we show the time domain solution of the compound system at 18.27 Hz and its spectrum in Figure 12(b). From the results it is possible again to see the dominant contribution of the first harmonic.

The other cases that present high amplitude solutions are: Neoprene at $T = 323, 313\,\text{K}$ and butyl rubber at $T = 323, 313, 273\,\text{K}$ in the cases with $f_0 = 10000$ and $\alpha = 5$. After a similar analysis of the numerical solution for these cases (not shown here) we obtained the same negligible contribution of the harmonics different from the first.

Summarizing, we can rely in the assumption of having only one harmonic in the solution and thus equation (15) gives the correct FRC of the considered system.

9. Conclusions

This work showed the influence of temperature on viscoelastic absorbers, designed to optimally control a cubic nonlinear single-d.f. system at the design temperature of 303 K. Two different real viscoelastic materials, which present interesting alternatives for vibration control purposes, were employed: butyl rubber and neoprene. The study was motivated due to the fact that viscoelastic materials are strongly influenced by temperature. This influence was also considered under

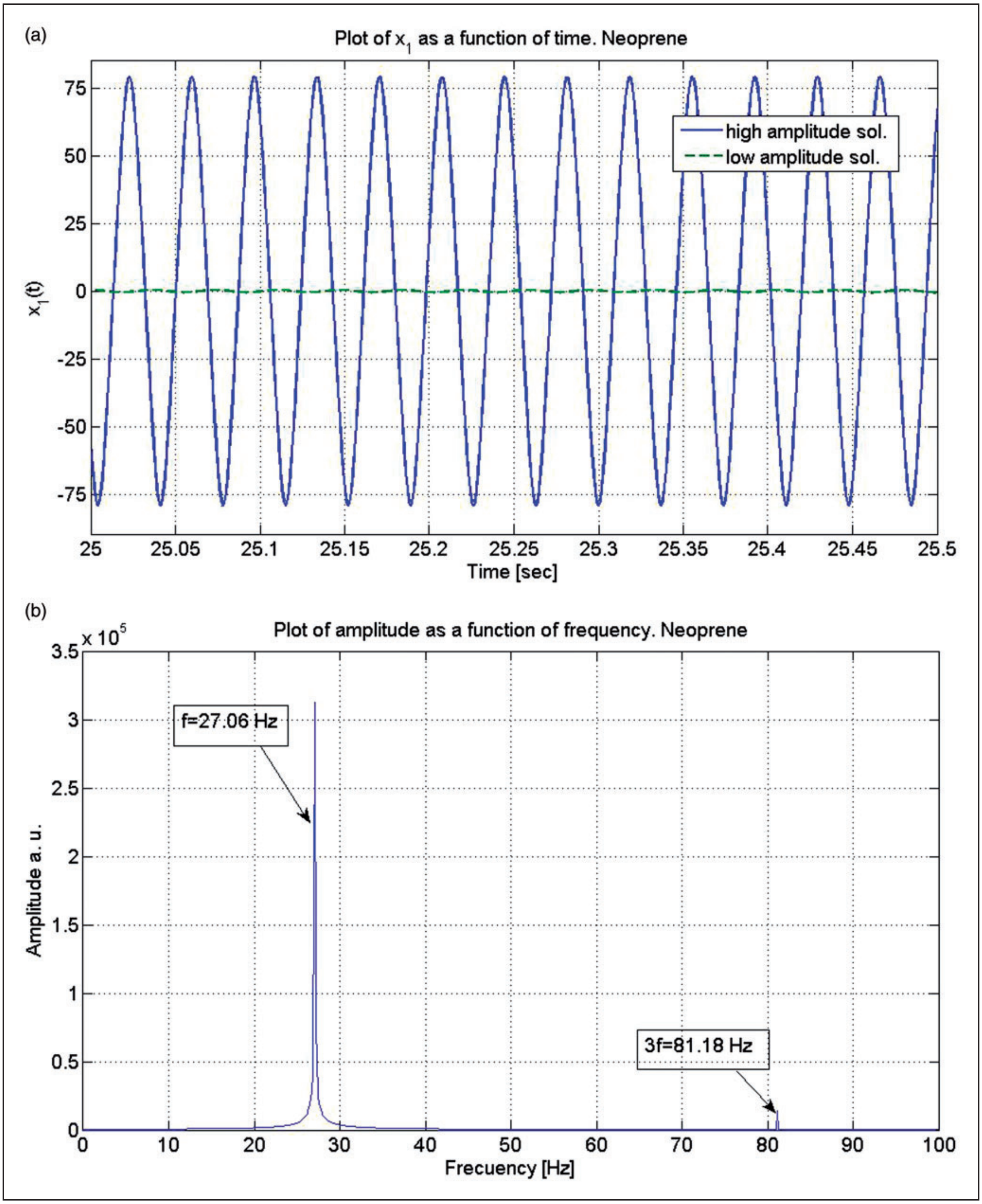

Figure 11. (a) Time response of the compound system with neoprene VDVA at $T = 333$ K, with $f_0 = 10000$, $\alpha = 5$ driven by a frequency of 27.06 Hz. The high amplitude solution (solid line) corresponds to the second upper arm in Figure 9(b) and the low amplitude solution (dotted line) is shown for comparison. (b) Spectrum of (a) high amplitude solution.

different external load amplitudes, or, equivalently, different non-linear behaviors.

The approach for modeling the compound system was introduced by the authors in a previous work and it was reviewed herein. It used the generalized equivalent parameter concept for the VDVA, which allowed the equations of motion of the compound system to be described in terms of the primary system coordinates only. The implementation of the optimization procedure was presented along with the mathematical formulation of the problem to obtain the steady-state solution. Then, the optimum

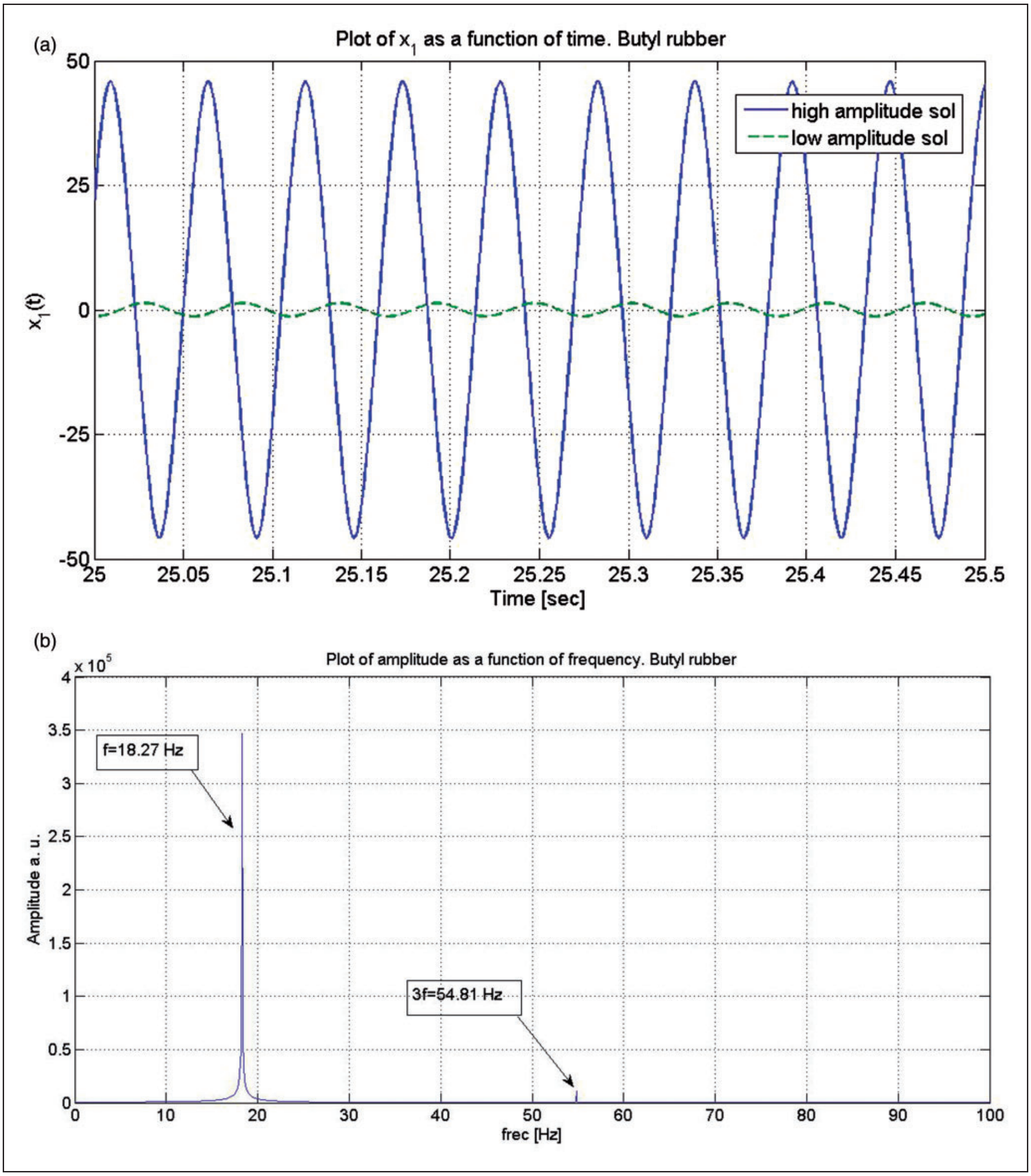

Figure 12. (a) Time response of the compound system with Butyl rubber VDVA at $T = 333$ K, with $f_0 = 10000$, $\alpha = 5$ driven by a frequency of 18.27 Hz. The high amplitude solution (solid line) corresponds to the second upper arm in Figure 10 and the low amplitude solution (dotted line) is shown for comparison. (b) Spectrum of (a).

parameters of the VDVA were recursively found for the different considered temperatures, which varied ± 30 K around the design temperature.

Generally speaking, the results showed that, when the temperature varies, the performance of the absorbers also modify, which was expected. However, this is not solely dependent on the temperature and the material characteristics but also on the magnitude of the excitation load imposed on the compound system.

For the neoprene VDVA and load magnitude $f_0 = 1000$, the compound system behaved as a damped linear two-d.f. system for the whole considered temperature range, presenting no severe detuning and keeping stability. In the other case of $f_0 = 10000$, the compound system remained stable only at 283 K and 293 K, showing jumps in the solutions for all the other temperatures.

For the butyl rubber VDVA and $f_0 = 1000$, a severe detuning was verified, deteriorating the performance of the absorber, especially at low temperatures, where the compound system even lost its stability. For $f_0 = 10000$, distortions around the peaks and jumps, characteristics of nonlinear behavior, were observed in the compound system for all the temperatures except in the design temperature.

From the stability analysis, the salient result was that no evidence of quasi-periodic motions due to Hopf bifurcations occurred for all the considered cases. Additionally, to account for the evidence of chaos, a large number of numerical simulations was performed, with several initial conditions, for all the considered cases and the whole set of corresponding frequencies. At the end of this procedure, no evidence of chaotic solutions was obtained.

Taking into account all the previous remarks, it can be concluded that, in terms of vibration control capabilities, the neoprene VDVA is less affected by a temperature variation than the butyl rubber VDVA, when a low magnitude of the excitation load is considered. On the other hand, a large load magnitude can significantly affect the performance of both absorbers when the working temperature is not the design temperature. In this case, a hybrid (passive-active) absorber, containing a viscoelastic material and an adaptive part, could be a convenient and interesting alternative.

Acknowledgments

M. Febbo acknowledges the financial support of CONICET, Universidad Nacional del Sur and Agencia Nacional de Promoción Científica y Técnica. E. M. O. Lopes and C. A. Bavastri acknowledge the financial support of CNPq.

Funding

This work was supported by Agencia Nacional de Promoción Científica y Técnica, Argentina (grant number PICT 2008 N°0423) and CONICET, Argentina (grant number PIP2010-2012 IP11220090100907).

References

Ashour ON and Nayfeh AH (2003) Experimental and numerical analysis of a nonlinear vibration absorber for the control of plate vibration. *Journal of Vibration and Control* 9: 209–234.

Bagley RL and Torvik PJ (1979) A generalized derivative model for an elastomeric damper. *The Shock and Vibration Bulletin* 49: 135–143.

Bagley RL and Torvik PJ (1983) A theoretical basis for application of fractional calculus to viscoelasticity. *Journal of Rheology* 27: 201–210.

Bagley RL and Torvik PJ (1986) On the fractional calculus model of viscoelastic behaviour. *Journal of Rheology* 30: 133–155.

Balthazar JM, Mook DT, Weber HI, Brasil RMLRF, Fenili A, Belato D and Felix JLP (2003) An overview on non-ideal vibrations. *Meccanica* 36(6): 613–621.

Bavastri CA (1997) *Vibration reduction in a large frequency band in complex structures using viscoelastic absorbers*. PhD thesis, Federal University of Santa Catarina, Brazil.

Bavastri CA, Espíndola JJ and Teixeira PH (1998) A hybrid algorithm to compute the optimal parameters of a system of viscoelastic vibration neutralizers in a frequency band. In *Proceedings of the Fourth International Conference on Motion and Vibration Control*, Zurich, Switzerland, 25–28 August, vol. 2, pp. 577–582.

Bavastri CA, Febbo M, Goncalves VV and Lopes EMO (2013) Optimum viscoelastic absorbers for cubic nonlinear systems. *Journal of Vibration and Control* 1–11. Doi 10.1177/1077546312473322.

Costa SNJ and Balthazar JM (2009) Suppression of vibrations in strongly nonhomogeneous 2DOF systems. *Nonlinear Dynamics* 58(4): 623–632.

Den Hartog JP (1956) *Mechanical Vibrations*. New York: McGraw-Hill.

DoubrawaFilho FJ, Luersen MA and Bavastri CA (2011) Optimal design of viscoelastic vibration absorbers for rotating systems. *Journal of Vibration and Control* 17: 699–710.

Espíndola JJ and Bavastri CA (1995) Modal reduction of vibrations by dynamic neutralizers in a frequency band–a generalized approach. In *Proceedings of the Sixth International Symposium on Dynamic Problems of Mechanics*, Caxambu, Minas Gerais, Brazil, 6–10 March, vol. 1, pp. 214–217.

Espíndola JJ and Bavastri CA (1997) Viscoelastic neutralizers in vibration abatement: a non-linear optimization approach. *Journal of The Brazilian Society of Mechanical Sciences* 19: 154–163.

Espíndola JJ and Silva HP (1992) Modal reduction of vibrations by dynamic neutralizers. In *Proceedings of the Tenth International Modal Analysis Conference*, San Diego, CA, 18–21 February 1992, pp. 1367–1373.

Espíndola JJ, Bavastri CA and Lopes EMO (2010) On the passive control of vibrations with viscoelastic dynamic absorbers of ordinary and pendulum types. *Journal of the Franklin Institute* 347: 102–115.

Espíndola JJ, Cruz GAM and Bavastri CA (2005a) On the design of optimum systems of viscoelastic vibration neutralizers. In: Hofer EP and Reithmeier E (eds) *Modelling and Control of Autonomous Decision Support Based Systems*. Aachen: Shaker Verlag, pp. 49–64.

Espíndola JJ, Silva Neto JM and Lopes EMO (2005b) On the fractional parameter identification of viscoelastic materials. In: Le Mehaueté A, Tenreiro Machado JA, Trigeassou JC and Sabatier J (eds) *Fractional Differentiation and its Applications*. Neusaess, Germany: Ubooks Verlag, pp. 327–340.

Espíndola JJ, Bavastri CA and Lopes EMO (2010) On the passive control of vibrations with viscoelastic dynamic absorbers of ordinary and pendulum types. *Journal of the Franklin Institute* 347(1): 102–115.

Espíndola JJ, Pereira P, Bavastri CA and Lopes EMO (2009) Design of optimum system of viscoelastic vibration absorbers with a Frobenius norm objective function. *Journal of the Brazilian Society of Mechanical Sciences and Engineering* 31(3): 210–219.

Espíndola JJ, Silva Neto JM and Lopes EMO (2005c) A generalized fractional derivative approach to viscoelastic material properties measurements. *Applied Mathematics and Computation* 164(2): 493–506.

Febbo M and Machado SP (2013) Nonlinear dynamic vibration absorbers with a saturation. *Journal of Sound and Vibration* 332(6): 1465–1483.

Ferry JD (1980) *Viscoelastic Properties of Polymers*. New York: JohnWiley and Sons.

Gendelman OV (2008) Targeted energy transfer in systems with non-polynomial nonlinearity. *Journal of Sound and Vibration* 315: 732–745.

Ji JC (2012) Application of a weakly nonlinear absorber to suppress the resonant vibrations of a forced nonlinear oscillator. *Journal of Vibration and Acoustics* 134(4): 044502–044502-6.

Ji JC and Zhang N (2010) Suppression of the primary resonance vibrations of a forced nonlinear system using a dynamic vibration absorber. *Journal of Sound and Vibration* 329(11): 2044–2056.

Kerschen G, Lee YS, Vakakis AF, McFarland DM and Bergman LA (2006) Irreversible passive energy transfer in coupled oscillators with essential nonlinearity. *SIAM Journal of Applied Mathematics* 66(2): 648–679.

Lopes EMO (1998) *On the experimental response reanalysis of structures with elastomeric materials*. PhD Thesis, University of Wales Cardiff, UK.

Nashif AD, Jones DIG and Henderson JP (1985) *Vibration Damping*. New York: John Wiley and Sons.

Natsiavas S (1992) Steady state oscillations and stability of non-linear dynamic vibration absorbers. *Journal of Sound and Vibration* 156(2): 227–245.

Nayfeh AH and Mook DT (1979) *Nonlinear Oscillations*. New York: John Wiley and Sons.

Neves PT Jr, Bavastri CA, Pereira JT, Oliveira RA, Pohl AAP, Boni DA and Luersen MA (2011) Fiber Bragg grating tuning with notch-type spring device. *Measurement Science and Technology* 22(8): 085303.

Nissen JC, Popp K and Schmalhorst B (1985) Optimization of a non-linear dynamic vibration absorber. *Journal of Sound and Vibration* 99(1): 149–154.

Nozaki R, Balthazar JM, Tusset AM, De Pontes BR Jr and Bueno AM (2013) Nonlinear control system applied to atomic force microscope including parametric errors. *Journal of Control, Automation and Electrical Systems* 24(3): 223–231.

Oueini SS, Char-Ming C and Nayfeh AH (2000) Response of two quadratically-coupled oscillators to a principal parametric excitation. *Journal of Vibration and Control* 6(7): 1115–1133.

Pipes LA (1953) Analysis of a non-linear dynamic vibration absorber. *Journal of Applied Mechanics* 20: 515–518.

Pritz T (1996) Analysis of four-parameter fractional derivative model of real solid materials. *Journal of Sound and Vibration* 195(1): 103–115.

Rice HJ (1986) Combination instability of the nonlinear vibration absorber. *Journal of Sound and Vibration* 108: 526–532.

Roberson RE (1952) Synthesis of a non-linear dynamic vibration absorber. *Journal of the Franklin Institute* 254: 205–220.

Rossikhin YA and Shitikova V (1998) Application of fractional calculus for analysis of nonlinear damped vibrations of suspension bridges. *Journal of Engineering Mechanics* 124(9): 1029–1036.

Schmidt G and Tondl A (1986) *Non-Linear Vibrations*. Cambridge: Cambridge University Press.

Shaw J, Shaw ST and Haddow AG (1989) On the response of the non-linear vibration absorber. *International Journal of Non-Linear Mechanics* 24(4): 281–293.

Silveira M, Pontes BR Jr and Balthazar JM (2014) Use of nonlinear asymmetrical shock absorber to improve comfort on passenger vehicles. *Journal of Sound and Vibration* 333(7): 2114–2129.

Snowdon JC (1968) *Vibration and Shock in Damped Mechanical Systems*. New York: John Wiley and Sons.

Soom A and Lee M (1983) Optimal design of linear and nonlinear vibration absorbers for damped systems. *Journal of Vibration, Acoustics, Stress and Reliability in Design* 105: 112–119.

Thomsen JJ (2010) *Vibrations and Stability*. Berlin: Springer-Verlag.

Torvik PJ and Bagley RL (1987) Fractional derivatives in the description of damping materials and phenomena: the role of damping in vibration and noise control. In *Proceedings of the Eleventh Biennial Conference on Mechanical Vibration and Noise*, Boston, MA, 27–30 September, pp. 125–135.

Tusset AM, Balthasar JM and Felix JLP (2013) On elimination of chaotic behaviour in a non-ideal portal frame structural system, using both passive and active controls. *Journal of Vibration and Control* 19(6): 803–813.

Vakakis AF, Gendelman OV, Bergman LA, McFarland DM, Kerschen G and Lee YS (2008) *Nonlinear Targeted Energy Transfer in Mechanical and Structural Systems*. Vols. 1 and 2, New York: Springer.

Worden K and Tomlinson GR (2001) *Nonlinearity in Structural Dynamics – Detection, Identification and Modelling*. Bristol: Institute of Physics Publishing.

Zhu SJ, Zheng YF and Fu YM (2004) Analysis of non-linear dynamics of a two-degree-of-freedom vibration system with non-linear damping and non-linear spring. *Journal of Sound and Vibration* 271: 15–24.